

## The structural requirements of HDAC inhibitors: SAHA analogs modified at the C2 position display HDAC6/8 selectivity

Ahmed T Negmeldin, Geetha Padige, Anton V Bieliauskas, and Mary Kay H. Pflum

ACS Med. Chem. Lett., **Just Accepted Manuscript** • DOI: 10.1021/acsmedchemlett.6b00124 • Publication Date (Web): 07 Feb 2017

Downloaded from <http://pubs.acs.org> on February 8, 2017

### Just Accepted

“Just Accepted” manuscripts have been peer-reviewed and accepted for publication. They are posted online prior to technical editing, formatting for publication and author proofing. The American Chemical Society provides “Just Accepted” as a free service to the research community to expedite the dissemination of scientific material as soon as possible after acceptance. “Just Accepted” manuscripts appear in full in PDF format accompanied by an HTML abstract. “Just Accepted” manuscripts have been fully peer reviewed, but should not be considered the official version of record. They are accessible to all readers and citable by the Digital Object Identifier (DOI®). “Just Accepted” is an optional service offered to authors. Therefore, the “Just Accepted” Web site may not include all articles that will be published in the journal. After a manuscript is technically edited and formatted, it will be removed from the “Just Accepted” Web site and published as an ASAP article. Note that technical editing may introduce minor changes to the manuscript text and/or graphics which could affect content, and all legal disclaimers and ethical guidelines that apply to the journal pertain. ACS cannot be held responsible for errors or consequences arising from the use of information contained in these “Just Accepted” manuscripts.

# The structural requirements of HDAC inhibitors: SAHA analogs modified at the C2 position display HDAC6/8 selectivity

Ahmed T. Negmeldin, Geetha Padige, Anton V. Bieliauskas,<sup>[a]</sup> Mary Kay H. Pflum\*

Department of Chemistry, Wayne State University, 5101 Cass Avenue, Detroit, MI 48202, United States

**KEYWORDS:** histone deacetylase, HDAC inhibitor, HDAC6 HDAC8 selective inhibitor, HDAC isoform selectivity, Vorinostat

**ABSTRACT:** Histone deacetylase (HDAC) proteins are epigenetic regulators that deacetylate protein substrates, leading to subsequent changes in cell function. HDAC proteins are implicated in cancers, and several HDAC inhibitors have been approved by the FDA as anti-cancer drugs, including SAHA (suberoylanilide hydroxamic acid, Vorinostat, Zolinza™). Unfortunately, SAHA inhibits most HDAC isoforms, which limits its use as a pharmacological tool and may lead to side effects in the clinic. In this work SAHA analogs substituted at the C2 position were synthesized and screened for HDAC isoform selectivity *in vitro* and in cells. The most potent and selective compound, C2-*n*-hexyl SAHA, displayed sub-micromolar potency with 49- to 300-fold selectivity for HDAC6 and HDAC8 compared to HDAC1, 2, and 3. Docking studies provided a structural rationale for selectivity. Modification of the non-selective inhibitor SAHA generated HDAC6/HDAC8 dual selective inhibitors, which can be useful lead compounds towards developing pharmacological tools and more effective anti-cancer drugs.

Histone deacetylase (HDAC) proteins play an important role in the epigenetic regulation of transcription. HDAC proteins deacetylate acetyllysine residues on nucleosomal histone proteins, which influences gene expression.<sup>1</sup> The HDAC family contains eighteen proteins, which are grouped into four classes according to their size, cellular localization, and phylogenetic analysis.<sup>2</sup> Classes I, II, and IV are metal dependent, while class III are NAD<sup>+</sup> dependent.<sup>2</sup> The metal dependent HDACs are the focus in this work.

Through the deacetylation of nucleosomal histones, HDAC proteins regulate both the expression and activity of cancer-related proteins that are involved in transcription, tumor suppression, and cell signaling.<sup>3-4</sup> Through the deacetylation of non-histone substrates, HDAC proteins affect protein stability, localization, and intracellular interactions, including protein-protein interactions and protein-DNA interactions.<sup>4-5</sup> Due to their fundamental role in regulating gene expression and protein activity, overexpression of HDAC proteins is linked to cancer formation.<sup>5</sup> For example, HDAC1 was overexpressed in prostate<sup>6</sup> and breast,<sup>7</sup> while HDAC8 has been implicated in neuroblastoma and T-cell lymphoma and acute myeloid leukemia.<sup>8</sup> Among the class II proteins, HDAC6 was overexpressed in oral squamous cell carcinoma.<sup>9</sup> In addition, HDAC6 is implicated in several non-epigenetic cancer-related intracellular functions.<sup>10</sup> Both HDAC6 and HDAC8 were found to be highly expressed and implicated in the invasion and progression of breast cancer cells.<sup>11</sup>

With a role in cancer, HDAC proteins have emerged as important targets for cancer treatment, with a wide variety of HDAC inhibitor drugs available.<sup>12-15</sup> The effect of HDAC inhibitors on both histone and non-histone proteins can lead to

cell signaling dysregulation, transcription and expression changes, and protein degradation. Through these effects on tumor cells, HDAC inhibitors can reduce proliferation, migration, and angiogenesis, enhance differentiation and immunogenicity, and promote apoptosis.<sup>16</sup> In fact, several HDAC inhibitors are used for treatment of T-cell lymphoma, including SAHA (suberoylanilide hydroxamic acid, Vorinostat, Figure 1) and Belinostat (Figure S41).<sup>12-14</sup> Panobinostat (Figure S41) was recently approved for treatment of multiple myeloma.<sup>15</sup> Unfortunately, these FDA approved drugs are relatively non-selective and inhibit most of the eleven metal-dependent HDAC isoforms.<sup>17</sup> Nonspecific inhibition may account for several mild to severe side effects associated with treatment, including dehydration, thrombocytopenia, anorexia, and cardiac arrhythmia.<sup>17-18</sup> In addition, the non-selectivity of these drugs limits their use as biological tools to probe HDAC function in cancer biology.

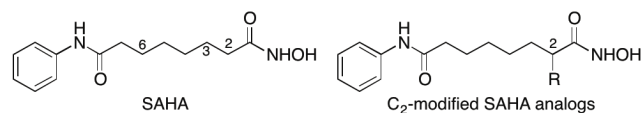


**Figure 1. Chemical structures of the FDA approved drug SAHA (suberoylanilide hydroxamic acid, Vorinostat, Zolinza™) and the C2-modified SAHA analogs reported here.**

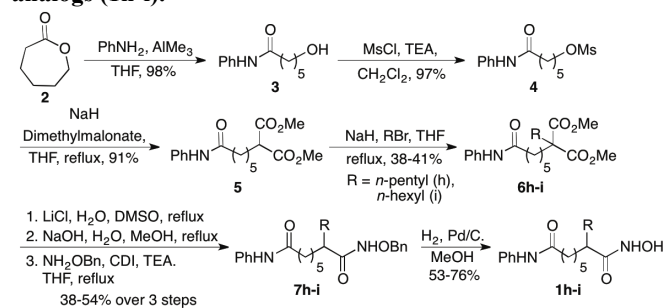
Several isoform selective inhibitors have been developed. MS-275 (Figure S41) is in clinical trials and is class I selective, with 4- to 400- fold selectivity for HDAC1, 2, and 3 over the other isoforms.<sup>17</sup> RGFP966 (Figure S41) showed more than 188-fold selectivity for HDAC3 over the other isoforms.<sup>19</sup> Tubastatin (Figure S41) is HDAC6 selective with 87-fold or 1000-fold selectivity for HDAC6 over HDAC1, 2, and 3 ac-

cording to different reports.<sup>20-21</sup> Selective inhibitors can be used as biological tools to elucidate the function of each isoform in the development of cancer. In addition, modification of non-selective inhibitors currently used in clinic can possibly improve their selectivity and reduce their clinical side effects.

Towards development of selective HDAC inhibitors, we previously created SAHA analogs containing substituents in the linker region between the hydroxamic acid and the anilide ends (Figure 1). A C3-modified SAHA analog showed modest preference for HDAC3, while C6-modified SAHA analogs displayed selectivity for HDAC1 and 6 compared to HDAC3.<sup>22-24</sup> In addition, modifying the amine of the hydroxamic acid reduced potency, but enhanced preference for HDAC1.<sup>25</sup> C2-modified SAHA analogs (Figure 1) were also generated and showed  $\mu\text{M}$  potency with HeLa cell lysates (Table S1), but no selectivity assessment was performed.<sup>22</sup> We report here a selectivity assessment of C2-modified SAHA analogs both *in vitro* and in cells. Modification at the C2 position led to reduced potency but enhanced selectivity compared to SAHA, with preference for HDAC6 and 8 over HDAC1, 2, and 3. HDAC6/8 dual inhibitors can be used as biological tools to study breast cancer metastasis.<sup>11, 26</sup> In addition, the SAHA analogs reported here are useful lead compounds for further development of pharmacological agents and anti-cancer drug targeting HDAC6 and 8. More generally, these studies confirm that modification of the SAHA linker region can enhance isoform selectivity.

**Synthesis of C2-modified SAHA analogs.** The syntheses of seven C2-modified SAHA analogs (**1a-g**) were previously described.<sup>22</sup> Two new derivatives, C2-*n*-pentyl SAHA (**1h**) and C2-*n*-hexyl SAHA (**1i**) are reported here. Synthesis began with ring opening of  $\epsilon$ -caprolactone **2** with aniline to give anilide alcohol **3**. Activation of the hydroxyl as a mesylate with subsequent substitution with dimethyl malonate gave intermediate diester **5**. Substitution with 1-bromopentane or 1-bromohexane generated the substituted diesters **6h-i**. Decarboxylation and subsequent saponification, followed by coupling with *N*-benzyl protected hydroxylamine afforded protected hydroxamic acids **7h-i**. Finally, hydrogenolysis gave the desired C2-*n*-pentyl (**1h**) and C2-*n*-hexyl SAHA (**1i**) analogs (Scheme 1).

#### Scheme 1. Synthesis of C2-*n*-pentyl and C2-*n*-hexyl SAHA analogs (**1h-i**).



***In-vitro* screening of C2-modified SAHA analogs.** Prior work showed that C2-modified SAHA analogs displayed weak  $\mu\text{M}$  potency with the HDAC activity from HeLa cell lysates.<sup>22</sup> However, no selectivity assessment was performed. In this work we used the recently developed ELISA-based HDAC activity assay to screen the analogs against mammalian-

derived HDAC1, HDAC2, HDAC3, and HDAC6.<sup>21</sup> As an initial test of selectivity, the potency of each C2-modified SAHA derivative was tested with HDAC1, 2, 3, and 6 at single concentrations of either 5 or 10  $\mu\text{M}$ . All analogs (**1a-i**) displayed some selectivity for HDAC6 compared to HDAC1, HDAC2, and HDAC3 (Figure 2). Among them, the C2-benzyl (**1g**), C2-*n*-pentyl (**1h**), and C2-*n*-hexyl (**1i**) analogs showed the greatest difference in inhibitory activity comparing HDAC6 to HDAC1, HDAC2, and HDAC3. In contrast, the C2-methyl SAHA analog was least selective, with similar activity against all four isoforms (Figure 2).

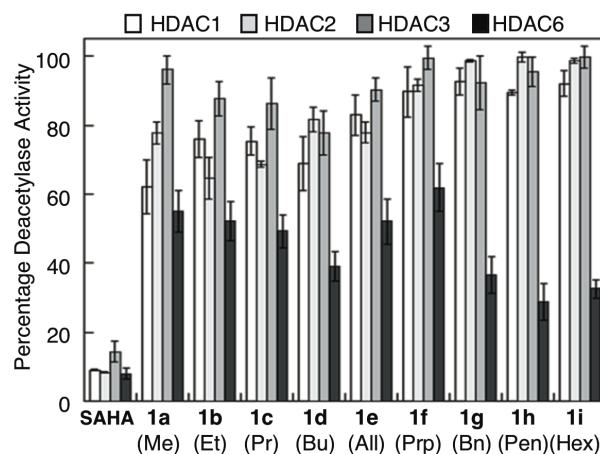


**Figure 2. Isoform selectivity screening of C2-modified SAHA analogs (**1a-i**) against HDAC1, 2, 3, and 6 using the ELISA-based HDAC activity assay.<sup>21</sup> All analogs were tested at 5  $\mu\text{M}$  concentration, except for **1d**, which was tested at 10  $\mu\text{M}$ . SAHA was tested at 1  $\mu\text{M}$ .<sup>21</sup> Mean percent deacetylase activities from a minimum of three independent trials with standard errors were plotted (Table S2). The substituent below each compound number corresponds to the R group in C2-modified SAHA (Figure 1).**

To further assess selectivity,  $\text{IC}_{50}$  values for the most selective compounds in the initial screen, compounds **1g-i**, were determined with HDAC1, 2, 3, 6, and 8 (Table 1). As controls, the  $\text{IC}_{50}$  values of both SAHA and tubastatin were included. As expected, SAHA displayed similar  $\text{IC}_{50}$  values with HDAC1-6, but 5-fold reduced activity with HDAC8, which is consistent with prior reports.<sup>17, 27</sup> Tubastatin showed at least 87-fold selectivity for HDAC6 over class I HDAC1, 2, and 3, but only 10-fold selectivity versus HDAC8.<sup>21</sup> Interestingly, the C2-modified SAHA analogs showed selectivity for HDAC6 and HDAC8, with  $\text{IC}_{50}$  values in the sub-micromolar to micromolar range (0.6-2.0  $\mu\text{M}$ , Table 1). The C2-benzyl **1g** and C2-*n*-pentyl **1h** analogs displayed 33 to 92-fold selectivity for HDAC6 and HDAC8 over the Class I isoforms (Tables 1, S5, and S6, and Figures S44 and S45). The most selective compound, C2-*n*-hexyl SAHA **1i** displayed 49- to 300-fold selectivity for HDAC6 and HDAC8 compared to the class I isoforms (Tables 1 and S7 and Figure S46).

It is notable that the selectivity of C2-*n*-hexyl SAHA **1i** for HDAC6 (>163-fold) is elevated compared to tubastatin (>87-fold), while it showed 20-fold less potency than tubastatin (0.60 vs. 0.031  $\mu\text{M}$   $\text{IC}_{50}$  values). The conclusion is that C2-substituents impart selectivity by discriminating against HDAC1, HDAC2, and HDAC3.

**Table 1.** IC<sub>50</sub> values for SAHA, Tubastatin, SAHA analogs **1g-1i** against HDAC1, 2, 3, 6, and 8.<sup>a</sup>

Compound	IC <sub>50</sub> values (μM)				
	HDAC1	HDAC2	HDAC3	HDAC6	HDAC8
SAHA <sup>21</sup>	0.033 ± 0.001	0.096 ± 0.01	0.020 ± 0.001	0.033 ± 0.003	0.54 ± 0.01
Tubastatin <sup>21</sup>	2.7 ± 0.2	3.9 ± 0.4	2.9 ± 0.5	0.031 ± 0.004	0.33 ± 0.01
<b>1g</b> (benzyl)	84 ± 6	110 ± 10	91 ± 4	1.5 ± 0.2	1.2 ± 0.1
<b>1h</b> (pentyl)	48 ± 2	58 ± 2	43 ± 2	0.85 ± 0.05	1.3 ± 0.1
<b>1i</b> (hexyl)	180 ± 20	180 ± 30	98 ± 10	0.60 ± 0.05	2.0 ± 0.1
<b>(S)-1i</b> (hexyl)	330 ± 30	580 ± 30	530 ± 50	ND	3.1 ± 0.1
<b>(R)-1i</b> (hexyl)	ND	ND	ND	ND	0.71 ± 0.01

<sup>a</sup> Mean IC<sub>50</sub> value and standard error of at least two independent trials are shown (Figures S42-S48 and Tables S3-S9). ND = not determined

**In-cell selectivity testing.** To assess the HDAC6 selectivities of the analogs in a biologically relevant context, C2-benzyl (**1g**), C2-*n*-pentyl (**1h**), and C2-*n*-hexyl (**1i**) SAHA were tested for their abilities to increase the acetylation levels of HDAC substrates. Acetylated- $\alpha$ -tubulin (AcTub) was monitored as a known substrate of HDAC6, whereas acetylated-histone H3 (AcH3) was observed as a substrate for HDAC1, 2, and 3. U937 myeloid leukemia cells were used in these cellular HDAC6 selectivity study. HDAC6 is overexpressed in several acute myeloid leukemia (AML) cell lines, suggesting that HDAC6 is a promising target for development of anti-leukemic drugs.<sup>28</sup> SAHA or the analogs were incubated with U937 cells before lysis and western blot analysis of protein acetylation. As expected, SAHA increased the acetylation levels of both  $\alpha$ -tubulin and histone H3 (Figure 3a, lane 2), consistent with its broad inhibition. In contrast, the HDAC6 selective inhibitor tubastatin affected only  $\alpha$ -tubulin acetylation (Figure 3a, lane 3). Similar to tubastatin, the three analogs **1h-i** increased acetylation levels of  $\alpha$ -tubulin to a greater level than histone H3 (Figure 3a, lanes 4-6). Quantification confirmed that **1h-i** significantly increased acetylation of  $\alpha$ -tubulin compared to DMSO, but not acetyl histone H3 levels (Figure 3b and Table S10). In addition, the C2-*n*-hexyl analog **1i** promoted a dose-dependent increase in acetylation of  $\alpha$ -tubulin, but not histone H3 (Figure 3c, lanes 2-7), compared to the DMSO control (Figure 3c, lane 1). The HDAC6-dependent acetylation of tubulin observed in cells is consistent with the HDAC6 selectivity observed *in-vitro* (Table 1 and Figure 2).

**Inhibitor cytotoxicity.** To test the anti-cytotoxic properties of the HDAC6-selective inhibitors, analogs **1g-i** were tested in cell-based cytotoxicity assays using leukemia cell lines.<sup>28</sup> First, the analogs were tested with the Jurkat cell line at 1 and 10  $\mu$ M concentrations using an MTT assay (Figure 4, Table S11). SAHA was also tested as a control. All compounds showed reduced cytotoxicity compared to the SAHA (Figure 4). Of the analogs, C2-*n*-hexyl SAHA (**1i**) showed the greatest cytotoxic effect, with only 47% viability at 10  $\mu$ M concentration.

To further assess cytotoxicity, both SAHA and the most potent analog **1i** were tested to determine EC<sub>50</sub> values against three leukemia cancer cell lines: Jurkat, AML MOLM-13, and U937 cells. SAHA showed potent cytotoxicity, with EC<sub>50</sub> values of 0.72, 1.2, and 0.88  $\mu$ M with Jurkat, AML MOLM-13, and U937 cell lines, respectively (Table 2). The observed EC<sub>50</sub> values are consistent with previous reports.<sup>29-31</sup>

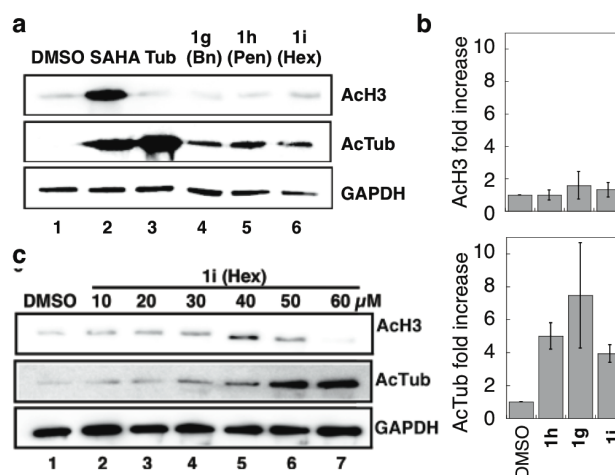


**Figure 3.** Cell-based selectivity testing of the SAHA analogs. U937 cells were treated with (a) DMSO (1%), SAHA (2  $\mu$ M), tubastatin (2  $\mu$ M), C2-benzyl SAHA (**1g**, 30  $\mu$ M), C2-*n*-pentyl SAHA (**1h**, 30  $\mu$ M), C2-*n*-hexyl SAHA (**1i**, 30  $\mu$ M), or (c) increasing concentrations of C2-*n*-hexyl SAHA analog (**1i**, 10-60  $\mu$ M) before lysis, SDS-PAGE separation, and western blot analysis of acetyl-histone H3 (AcH3) and acetyl- $\alpha$ -tubulin (AcTub). GAPDH was a load control. Repetitive trials are shown in Figures S49 and S50. (b) Fold increase in AcH3 or AcTub after quantification of bands intensity from part a, with mean fold increase from four independent trials and standard error (Table S10).

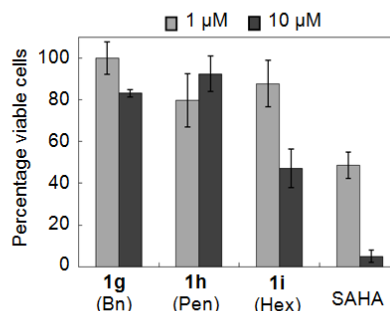


**Figure 4.** Cytotoxicity screening of **1g**, **1h**, **1i**, and SAHA at 1 and 10  $\mu$ M concentrations using an MTT assay with Jurkat cells. Mean percent viability from at least three independent trials with standard error were plotted (Table S11).

The high potency of SAHA may be due to its non-selectivity, as well as the high inhibitory activity against class 1 HDAC1, 2, and 3. The C2-*n*-hexyl SAHA analog **1i** showed roughly 10-fold reduced cytotoxicity compared to SAHA, with EC<sub>50</sub> values of 11.8, 10.5, and 13.8 μM with Jurkat, AML MOLM-13, and U937 cell lines, respectively (Table 2). The reduced cytotoxicity is consistent with the 18-fold reduction in potency against HDAC6 compared to SAHA (Table 1). In addition, the selectivity for HDAC6 and 8 over HDAC1, 2, and 3, might also contribute to the lower cytotoxicity.

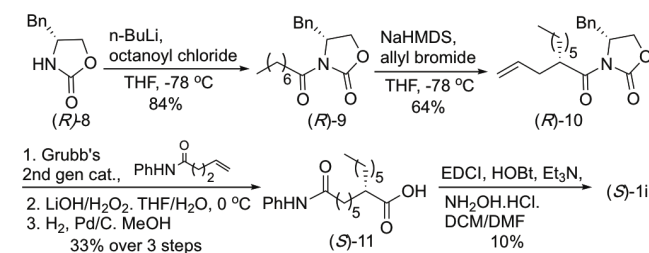
**Table 2: EC<sub>50</sub> values for SAHA and C2-*n*-hexyl (**1i**) SAHA analog against Jurkat, AML MOLM-13, and U937 cells using MTT assay.<sup>a</sup>**

Compound	Cellular EC <sub>50</sub> values (μM)		
	Jurkat	AML MOLM-13	U937
SAHA	0.72 ± 0.13	1.2 ± 0.06	0.88 ± 0.13
<b>1i</b> (hexyl)	11.8 ± 2.2	10.5 ± 3.1	13.8 ± 1.7

<sup>a</sup> Mean EC<sub>50</sub> value and standard error of at least three independent trials are shown (Figures S51-S52 and Tables S12-S13).

**Synthesis and Screening of (*R*)- and (*S*)-C2-*n*-hexyl SAHA (**1i**).** C2-*n*-hexyl SAHA (**1i**) contains a stereocenter at the 2 position and the compounds tested to this point were racemic mixtures. To test the selectivity of each enantiomer, an enantioselective synthesis of C2-*n*-hexyl SAHA (**1i**) was employed using Evans chiral auxiliary **8** and octanoyl chloride (Schemes 2 and S1). Allyl bromide was added to the resulting amide **9** to generate chiral compound (*R*)-**10** from auxiliary (*R*)-**8** (Scheme 2) or (*S*)-**10** from auxiliary (*S*)-**8** (Scheme S1). After olefin metathesis with Grubbs' second generation catalyst<sup>32</sup> and removal of the auxiliary, the olefin was reduced to generate (*S*)-**11** and (*R*)-**11**. Finally, coupling with hydroxylamine generated the two enantiomers of C2-*n*-hexyl SAHA, (*S*)-**1i** or (*R*)-**1i** in 95 and 92% ee, respectively.

Scheme 2. Synthesis of (*S*)-C2-*n*-hexyl SAHA, (**1i**).



With the two C2-*n*-hexyl SAHA enantiomers in hand, IC<sub>50</sub> values were determined (Table 1). As expected, both enantiomers displayed low micromolar to submicromolar potency with HDAC8 (3.1±0.1 or 0.71±0.01 μM), similar to racemic **1i** (2.0±0.1). The data suggested that (*R*)-**1i** is more potent than (*S*)-**1i**, although only by 4-fold. The (*S*)-**1i** enantiomer was further tested for selectivity against HDAC 1, 2, and 3. (*S*)-**1i** displayed 106- to 187-fold selectivity for HDAC8, which is greater than that observed with racemic **1i** (49- to 300-fold). In total, studies with the enantiomers of C2-*n*-hexyl SAHA indicated that both are low micromolar to submicromolar potency HDAC8 inhibitors, with the expected HDAC8 selectivity compared to HDAC1, 2, and 3.

**Docking studies.** To rationalize the HDAC6 selectivity of the C2-*n*-hexyl SAHA (**1i**) analog, we performed docking analysis using the AutoDock 4.2 program.<sup>33</sup> Both enantiomers of the analog were docked into the recently published HDAC6 crystal structure (pdb: 5EEM)<sup>34</sup> and both displayed similar binding interactions (Figure 5 and Figure S53), consistent with the similar IC<sub>50</sub> values observed experimentally. For example, the hydroxamic acid was positioned in bonding distance (1.9-2.9 Å) of three active site residues (H573, H574, and Y745) and the catalytic zinc atom in HDAC6 active site (Figures 5a and S53A). For comparison, docking of the parent SAHA compound with HDAC6 showed similar distances between the hydroxamic acid and the active site (1.6-2.4 Å, Figure S54A). To explore the HDAC6 selectivity, compound **1i** was also docked into the HDAC2 crystal structure (pdb ID: 3MAX).<sup>35</sup> In contrast to the bonding distances observed with HDAC6, elongated distances between the hydroxamic acid group and H145 (5.7-5.9 Å), H146 (3.8 Å), and Y308 (3.0-5.5 Å) were observed (Figures 5b and S53B). Metal binding was also weakened with longer bond distances (3.5-4.7 Å, Figures 5b and S53B). One possibility accounting for the weak binding with HDAC2 is that the bulky C2-*n*-hexyl substituent cannot favorably fit into the relatively narrow catalytic active channel of HDAC2.<sup>20</sup> Consistent with this possibility, superimposition of the docked poses of compound **1i** and SAHA with HDAC2 showed that the C2-*n*-hexyl substituent is positioned towards the solvent exposed surface of the active site, which consequently places the hydroxamic acid distant from the metal (Figure S55C and D). In contrast, the relatively wide catalytic pocket in HDAC6 allowed compound **1i** and SAHA to similarly position the hydroxamic acid within bonding distances of the catalytic metal and nearby residues (Figure S55A and B).

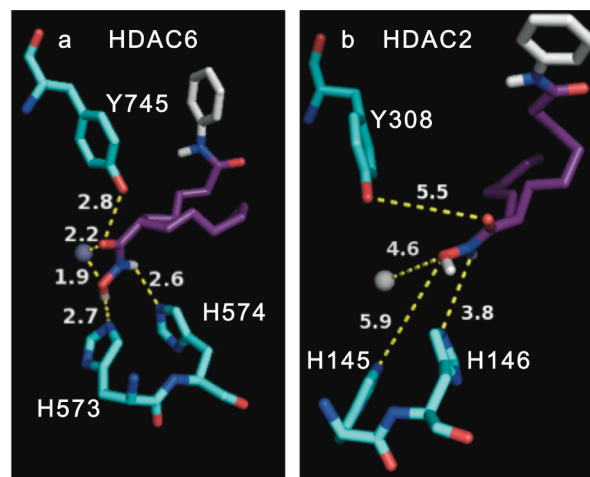


**Figure 5. Docked pose of (*S*)-C2-*n*-hexyl SAHA ((*S*)-**1i**) in the (a) HDAC6 (pdb:5EEM)<sup>34</sup> or (b) HDAC2 (pdb:3MAX)<sup>35</sup> crystal structures (b) using Autodock 4.2.<sup>33</sup> Binding distances between the hydroxamic acid atoms and active site residues (numbered in figure) or the metal are displayed in Angstroms. The (*R*) enantiomer is shown in Figure S53. The atomic radius of the metal (Zn<sup>2+</sup>) was set at 0.5 Å for clarity. Atom color-coding: (*S*)-C2-*n*-hexyl SAHA (C=purple/white; O=red; N=blue; H=white); amino acids (C=deep teal; O=red, N=blue); Zn<sup>2+</sup> metal ion (grey sphere).**

Because all HDAC isoforms show high conservation among their active site residues,<sup>36-37</sup> previous studies suggested that the shape of the active sites might explain the HDAC6 selectivity of reported compounds.<sup>38</sup> In particular, HDAC6 maintains a wider active site entrance compared to the class I isoforms.<sup>20</sup> In previous work, HDAC6-selective inhibitors were generated by replacing the solvent-exposed anilide group of SAHA with bulky aryl groups.<sup>20, 39-40</sup> In addition, compounds with an aryl, cyclic, or unsaturated group attached in the linker region directly adjacent to the hydroxamic acid demonstrated HDAC6 selectivity.<sup>40</sup> For example, tubastatin is a highly HDAC6-selective inhibitor that displays a series of bulky aryl groups near the hydroxamic acid (Figure S41).<sup>20</sup> More closely related to this work, valpropylhydroxamic acid (Figure S41) positions an alkyl group adjacent to a hydroxamic acid and showed HDAC6/8 dual selectivity, with 16 and 39  $\mu\text{M}$   $\text{IC}_{50}$  against HDAC6 and 8, respectively, but only 9-17-fold reduced potency with HDAC1, 2, and 3.<sup>41</sup> The data with valpropylhydroxamic acid are consistent with our data showing that the linker can influence potency and selectivity. Our docking analysis and these prior studies suggest that the selectivity of the C2-modified SAHA analogs is due to the bulky substituent adjacent to the hydroxamic acid takes advantage of the wider active site entrance of HDAC6 and HDAC8.<sup>20, 42</sup>

In conclusion, we report the synthesis and screening of several SAHA analogs substituted at the C2 position. C2-modified SAHA analogs displayed selectivity for HDAC6 and HDAC8 over HDAC1, 2, and 3. The highest selectivity observed was with C2-*n*-hexyl SAHA analog **1i**, which displayed 49- to 300-fold selectivity for HDAC6 and 8 over HDAC1, 2, and 3. Importantly, the selectivity of C2-*n*-hexyl SAHA is elevated compared to the widely used HDAC6-selective inhibitor, tubastatin. Cell-based selectivity testing of analogs **1g-i** reproduced the selectivity observed *in vitro*. The dual HDAC6/8 selective C2-modified SAHA analogs reported in this work can be useful as lead compounds to develop pharmacological tools and anti-cancer drugs targeting HDAC6 and HDAC8. More generally, these studies with SAHA analogs suggest that modifying known drugs can significantly improve their properties.

## ASSOCIATED CONTENT

### Supporting Information

The Supporting Information is available free of charge on the ACS Publications website. Experimental procedure, procedure for biological screening, docking procedure, compound characterization,  $\text{IC}_{50}$  curves and tables, and docking figures. (PDF)

## AUTHOR INFORMATION

### Corresponding Author

\* Phone: 313-577-1515; Fax: States Fax: 313-577-8822;  
E-mail: pflum@wayne.edu

### Present Addresses

[a] Dr. A.V. Bieliauskas, Ash Stevens, Inc., 18655 Krause Street, Riverview, MI 48193

### Author Contributions

A.T.N purified and tested compounds **1g-i** and performed all in cells selectivity, cytotoxicity, and docking studies. G.P. tested compounds **1a-f**. A.V.B. synthesized analogs (**1a-i**), while A.T.N

synthesized (**S**)-**1i** and (**R**)-**1i**. M.K.H.P. conceived of the project and assisted in experimental design and interpretation. All authors contributed to the writing of the manuscript.

## Funding Sources

We thank National Institutes of Health (GM067657) and Wayne State University for funding. The content is solely the responsibility of the authors and does not necessarily represent the official views of the National Institutes of Health.

## Notes

The authors declare no competing financial interest.

## ACKNOWLEDGMENT

We thank the Lumigen Instrument Center at Wayne State University for NMR and MS instrumentation, Dr. Y. Ge for the AML MOLM-13, and U937 cell lines, Dr. K. Honn for use of the Alpha Innotech FluorChem imaging system, Dr. M. Allen for use of the chiral HPLC column, Dr. Y. Danylyuk for HRMS analysis, and Dr. D. Nalawansa for helpful comments.

## ABBREVIATIONS

HDAC, histone deacetylase; SAHA, suberoylanilide hydroxamic acid; NAD, Nicotinamide adenine dinucleotide; DNA, deoxyribonucleic acid; FDA, Food and Drug Administration; ELISA, enzyme-linked immunosorbent assay; SDS-PAGE, sodium dodecyl sulfate polyacrylamide gel electrophoresis; GAPDH, Glyceraldehyde 3-phosphate dehydrogenase; AML, Acute Myeloid Leukemia; MTT, 3-(4,5-Dimethylthiazol-2-yl)-2,5-Diphenyltetrazolium Bromide; CDI, carbonyldiimidazole; TEA, triethylamine; EDCI, N-(3-Dimethylaminopropyl)-N'-ethylcarbodiimide hydrochloride; NaHMDS, Sodium bis(trimethylsilyl)amide; DCM, Dichloromethane.

## REFERENCES

- Walsh, C. T.; Gameau-Tsodikova, S.; Gatto, G. J., Protein posttranslational modifications: the chemistry of proteome diversifications. *Angew. Chem., Int. Ed.* **2005**, *44* (45), 7342-7372.
- Gregoretto, I.; Lee, Y.-M.; Goodson, H. V., Molecular evolution of the histone deacetylase family: functional implications of phylogenetic analysis. *J. Mol. Biol.* **2004**, *338* (1), 17-31.
- Glozak, M. A.; Seto, E., Histone deacetylases and cancer. *Oncogene* **2007**, *26* (37), 5420-32.
- Chuang, C.; Pan, J.; Hawke, D. H.; Lin, S.-H.; Yu-Lee, L.-y., NudC deacetylation regulates mitotic progression. *PLoS ONE* **2013**, *8* (9), e73841.
- Newbold, A.; Salmon, J. M.; Martin, B. P.; Stanley, K.; Johnstone, R. W., The role of p21waf1/cip1 and p27Kip1 in HDAC-mediated tumor cell death and cell cycle arrest in the E[ $\mu$ ]-myc model of B-cell lymphoma. *Oncogene* **2014**, *33* (47), 5415-5423.
- Halkidou, K.; Gaughan, L.; Cook, S.; Leung, H. Y.; Neal, D. E.; Robson, C. N., Upregulation and nuclear recruitment of HDAC1s in hormone refractory prostate cancer. *Prostate* **2004**, *59* (2), 177-189.
- Zhang, Z.; Yamashita, H.; Toyama, T.; Sugiura, H.; Ando, Y.; Mita, K.; Hamaguchi, M.; Hara, Y.; Kobayashi, S.; Iwase, H., Quantitation of HDAC1 mRNA expression in invasive carcinoma of the breast. *Breast Cancer Res. Treat.* **2005**, *94* (1), 11-6.
- Oehme, I.; Deubzer, H. E.; Wegener, D.; Pickert, D.; Linke, J.-P.; Hero, B.; Kopp-Schneider, A.; Westermann, F.; Ulrich, S. M.; von Deimling, A.; Fischer, M.; Witt, O., Histone deacetylase 8 in neuroblastoma tumorigenesis. *Clin. Cancer Res.* **2009**, *15* (1), 91-99.
- Sakuma, T.; Uzawa, K.; Onda, T.; Shiiba, M.; Yokoe, H.; Shibahara, T.; Tanzawa, H., Aberrant expression of histone

deacetylase 6 in oral squamous cell carcinoma. *Int. J. Oncol.* **2006**, *29* (1), 117-24.

(10) Aldana-Masangkay, G. I.; Sakamoto, K. M., The role of HDAC6 in cancer. *J. Biomed. Biotechnol.* **2011**, *2011*, 875824.

(11) Park, S. Y.; Jun, J. A.; Jeong, K. J.; Heo, H. J.; Sohn, J. S.; Lee, H. Y.; Park, C. G.; Kang, J., Histone deacetylases 1, 6 and 8 are critical for invasion in breast cancer. *Oncology reports* **2011**, *25* (6), 1677-81.

(12) Warrell, R. P., Jr.; He, L. Z.; Richon, V.; Calleja, E.; Pandolfi, P. P., Therapeutic targeting of transcription in acute promyelocytic leukemia by use of an inhibitor of histone deacetylase. *J. Natl. Cancer Inst.* **1998**, *90* (21), 1621-1625.

(13) Grant, S.; Easley, C.; Kirkpatrick, P., Vorinostat. *Nat. Rev. Drug Discovery* **2007**, *6* (1), 21-22.

(14) Plumb, J. A.; Finn, P. W.; Williams, R. J.; Bandara, M. J.; Romero, M. R.; Watkins, C. J.; La Thangue, N. B.; Brown, R., Pharmacodynamic response and inhibition of growth of human tumor xenografts by the novel histone deacetylase inhibitor PXD101. *Mol. Cancer Ther.* **2003**, *2* (8), 721-728.

(15) Laubach, J. P.; Moreau, P.; San-Miguel, J. F.; Richardson, P. G., Panobinostat for the treatment of multiple myeloma. *Clin. Cancer Res.* **2015**, *21* (21), 4767-4773.

(16) West, A. C.; Johnstone, R. W., New and emerging HDAC inhibitors for cancer treatment. *J. Clin. Invest.* **2014**, *124* (1), 30-39.

(17) Khan, N.; Jeffers, M.; Kumar, S.; Hackett, C.; Boldog, F.; Khramtsov, N.; Qian, X.; Mills, E.; Berghs, S. C.; Carey, N.; Finn, P. W.; Collins, L. S.; Tumber, A.; Ritchie, J. W.; Jensen, P. B.; Lichenstein, H. S.; Sehested, M., Determination of the class and isoform selectivity of small-molecule histone deacetylase inhibitors. *Biochem. J.* **2008**, *409* (2), 581-589.

(18) Kelly, W. K.; O'Connor, O. A.; Krug, L. M.; Chiao, J. H.; Heaney, M.; Curley, T.; MacGregore-Cortelli, B.; Tong, W.; Secrist, J. P.; Schwartz, L.; Richardson, S.; Chu, E.; Olgac, S.; Marks, P. A.; Scher, H.; Richon, V. M., Phase I study of an oral histone deacetylase inhibitor, suberoylanilide hydroxamic acid, in patients with advanced cancer. *J. Clin. Oncol.* **2005**, *23* (17), 3923-3931.

(19) Malvaez, M.; McQuown, S. C.; Rogge, G. A.; Astarabadi, M.; Jacques, V.; Carreiro, S.; Rusche, J. R.; Wood, M. A., HDAC3-selective inhibitor enhances extinction of cocaine-seeking behavior in a persistent manner. *Proc. Natl. Acad. Sci. U. S. A.* **2013**, *110* (7), 2647-2652.

(20) Butler, K. V.; Kalin, J.; Brochier, C.; Vistoli, G.; Langley, B.; Kozikowski, A. P., Rational design and simple chemistry yield a superior, neuroprotective HDAC6 inhibitor, tubastatin A. *J. Am. Chem. Soc.* **2010**, *132* (31), 10842-10846.

(21) Padige, G.; Negmeldin, A. T.; Pflum, M. K. H., Development of an ELISA-based HDAC activity assay for characterization of isoform-selective inhibitors. *J. Biomol. Screening* **2015**, *20* (10), 1277-1285.

(22) Bieliauskas, A.; Weerasinghe, S.; Pflum, M. H., Structural requirements of HDAC inhibitors: SAHA analogs functionalized adjacent to the hydroxamic acid. *Bioorg. Med. Chem. Lett.* **2007**, *17* (8), 2216-2219.

(23) Choi, S. E.; Weerasinghe, S. V.; Pflum, M. K., The structural requirements of histone deacetylase inhibitors: Suberoylanilide hydroxamic acid analogs modified at the C3 position display isoform selectivity. *Bioorg. Med. Chem. Lett.* **2011**, *21* (20), 6139-6142.

(24) Choi, S. E.; Pflum, M. K. H., The structural requirements of histone deacetylase inhibitors: Suberoylanilide hydroxamic acid analogs modified at the C6 position. *Bioorg. Med. Chem. Lett.* **2012**, *22* (23), 7084-7086.

(25) Bieliauskas, A. V.; Weerasinghe, S. V. W.; Negmeldin, A. T.; Pflum, M. K. H., Structural requirements of histone deacetylase inhibitors: SAHA analogs modified on the hydroxamic acid. *Arch. Pharm. (Weinheim, Ger.)* **2016**, *349*.

(26) Olson, D. E.; Wagner, F. F.; Kaya, T.; Gale, J. P.; Aidoud, N.; Davoine, E. L.; Lazzaro, F.; Weiwer, M.; Zhang, Y. L.; Holson, E. B., Discovery of the first histone deacetylase 6/8 dual inhibitors. *J. Med. Chem.* **2013**, *56* (11), 4816-4820.

(27) Bradner, J. E.; West, N.; Grachan, M. L.; Greenberg, E. F.; Haggarty, S. J.; Warnow, T.; Mazitschek, R., Chemical phylogenetics of histone deacetylases. *Nat. Chem. Biol.* **2010**, *6* (3), 238-243.

(28) Hackanson, B.; Rimmele, L.; Benkiser, M.; Abdelkarim, M.; Fliegau, M.; Jung, M.; Lübbert, M., HDAC6 as a target for antileukemic drugs in acute myeloid leukemia. *Leuk. Res.* **2012**, *36* (8), 1055-1062.

(29) Vickers, C. J.; Olsen, C. A.; Leman, L. J.; Ghadiri, M. R., Discovery of HDAC inhibitors that lack an active site Zn<sup>2+</sup>-binding functional group. *ACS Med. Chem. Lett.* **2012**, *3* (6), 505-508.

(30) Sodji, Q. H.; Patil, V.; Kornacki, J. R.; Mrksich, M.; Oyelere, A. K., Synthesis and structure-activity relationship of 3-hydroxypyridine-2-thione-based histone deacetylase inhibitors. *J. Med. Chem.* **2013**, *56* (24), 9969-9981.

(31) Li, X.; Inks, E. S.; Li, X.; Hou, J.; Chou, C. J.; Zhang, J.; Jiang, Y.; Zhang, Y.; Xu, W., Discovery of the first N-hydroxycinnamamide-based histone deacetylase 1/3 dual inhibitors with potent oral antitumor activity. *J. Med. Chem.* **2014**, *57* (8), 3324-3341.

(32) Chatterjee, A. K.; Choi, T.-L.; Sanders, D. P.; Grubbs, R. H., A General Model for Selectivity in Olefin Cross Metathesis. *J. Am. Chem. Soc.* **2003**, *125* (37), 11360-11370.

(33) Morris, G. M.; Huey, R.; Lindstrom, W.; Sanner, M. F.; Belew, R. K.; Goodsell, D. S.; Olson, A. J., AutoDock4 and AutoDockTools4: automated docking with selective receptor flexibility. *J. Comput. Chem.* **2009**, *30* (16), 2785-2791.

(34) Hai, Y.; Christianson, D. W., Histone deacetylase 6 structure and molecular basis of catalysis and inhibition. *Nat. Chem. Biol.* **2016**, *12* (9), 741-747.

(35) Bressi, J. C.; Jennings, A. J.; Skene, R.; Wu, Y.; Melkus, R.; Jong, R. D.; O'Connell, S.; Grimshaw, C. E.; Navre, M.; Gangloff, A. R., Exploration of the HDAC2 foot pocket: synthesis and SAR of substituted N-(2-aminophenyl)benzamides. *Bioorg. Med. Chem. Lett.* **2010**, *20* (10), 3142-3145.

(36) Weerasinghe, S. V. W.; Estiu, G.; Wiest, O.; Pflum, M. K. H., Residues in the 11Å channel of histone deacetylase 1 promote catalytic activity: Implications for designing isoform-selective histone deacetylase inhibitors. *J. Med. Chem.* **2008**, *51* (18), 5542-5551.

(37) Wambua, M. K.; Nalawansa, D. A.; Negmeldin, A. T.; Pflum, M. K., Mutagenesis studies of the 14 Å internal cavity of histone deacetylase 1: Insights towards the acetate escape hypothesis and selective inhibitor design. *J. Med. Chem.* **2014**, *57* (3), 642-650.

(38) Estiu, G.; Greenberg, E.; Harrison, C. B.; Kwiatkowski, N. P.; Mazitschek, R.; Bradner, J. E.; Wiest, O., Structural origin of selectivity in class II-selective histone deacetylase inhibitors. *J. Med. Chem.* **2008**, *51* (10), 2898-2906.

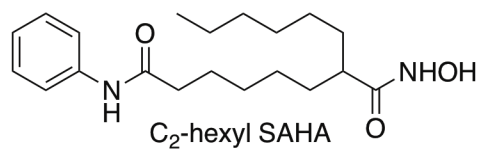
(39) Kozikowski, A. P.; Chen, Y.; Gaysin, A. M.; Savoy, D. N.; Billadeau, D. D.; Kim, K. H., Chemistry, biology, and QSAR studies of substituted biaryl hydroxamates and mercaptoacetamides as HDAC inhibitors-nanomolar-potency inhibitors of pancreatic cancer cell growth. *ChemMedChem* **2008**, *3* (3), 487-501.

(40) Wagner, F. F.; Olson, D. E.; Gale, J. P.; Kaya, T.; Weiwer, M.; Aidoud, N.; Thomas, M.; Davoine, E. L.; Lemerrier, B. C.; Zhang, Y. L.; Holson, E. B., Potent and selective inhibition of histone deacetylase 6 (HDAC6) does not require a surface-binding motif. *J. Med. Chem.* **2013**, *56* (4), 1772-1776.

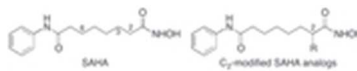
(41) Fass, D. M.; Shah, R.; Ghosh, B.; Hennig, K.; Norton, S.; Zhao, W.-N.; Reis, S. A.; Klein, P. S.; Mazitschek, R.; Maglathlin, R. L.; Lewis, T. A.; Haggarty, S. J., Short-chain HDAC inhibitors differentially affect vertebrate development and neuronal chromatin. *ACS Med. Chem. Lett.* **2011**, *2* (1), 39-42.

(42) KrennHrubec, K.; Marshall, B. L.; Hedglin, M.; Verdin, E.; Ulrich, S. M., Design and evaluation of 'Linkerless' hydroxamic acids as selective HDAC8 inhibitors. *Bioorg. Med. Chem. Lett.* **2007**, *17* (10), 2874-2878.

## Table of Contents Graphic



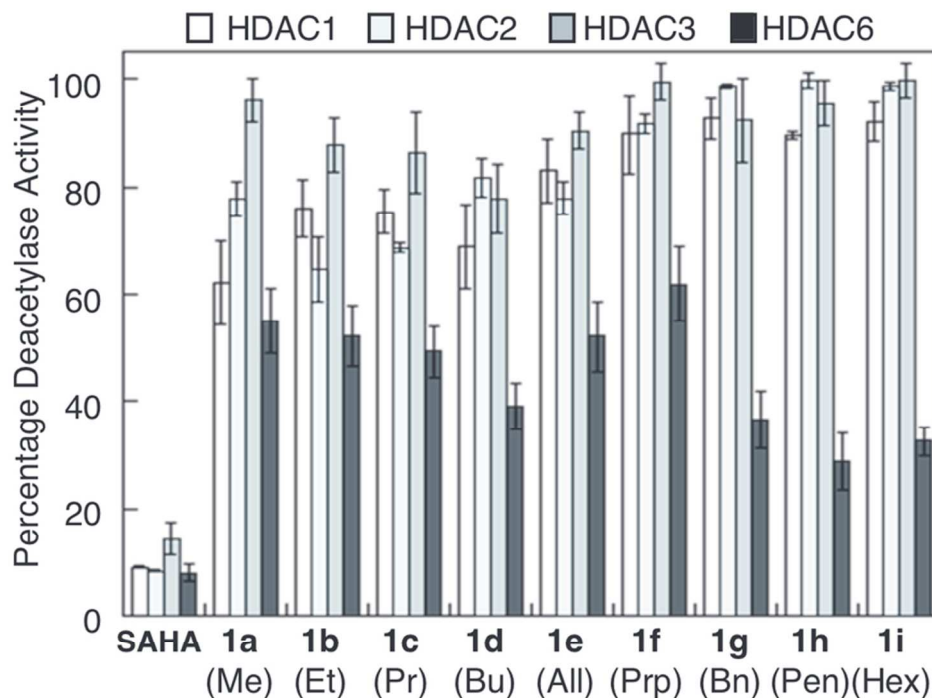
HDAC1 IC <sub>50</sub> = 180 μM	} 49- to 300- fold dual HDAC6/8 selectivity
HDAC2 IC <sub>50</sub> = 180 μM	
HDAC3 IC <sub>50</sub> = 98 μM	
HDAC6 IC <sub>50</sub> = 0.60 μM	
HDAC8 IC <sub>50</sub> = 2.0 μM	



Chemical structures of the FDA approved drug SAHA (suberoylanilide hydroxamic acid, Vorinostat, Zolinza™) and the C<sub>2</sub>-modified SAHA analogs reported here

Figure 1

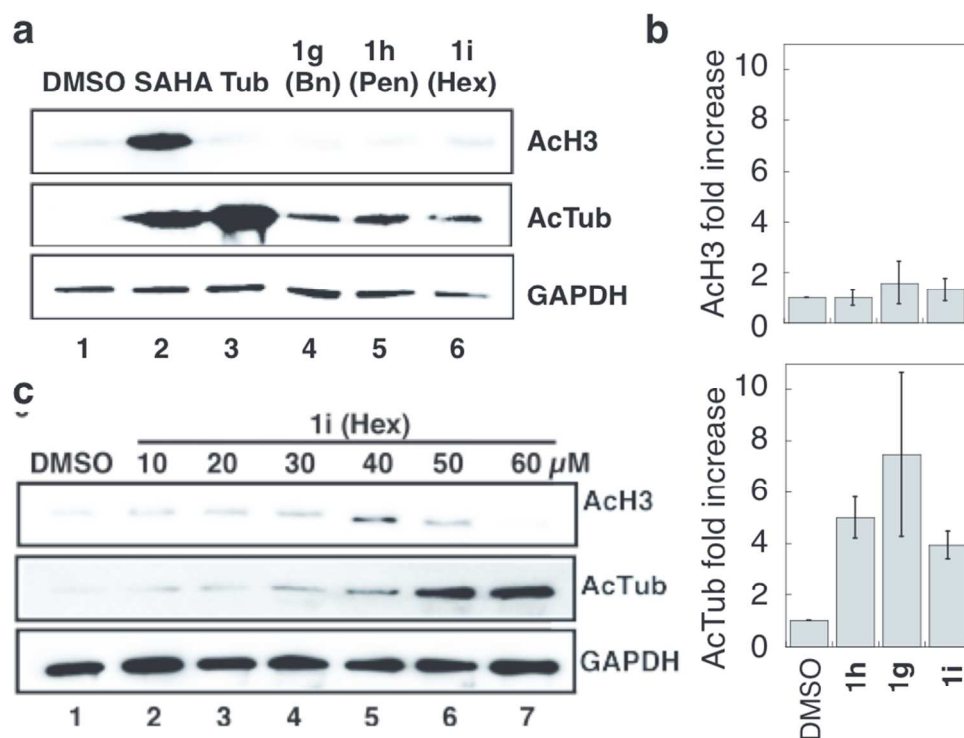
15x2mm (300 x 300 DPI)



Isoform selectivity screening of C2-modified SAHA analogs (1a-i) against HDAC1, 2, 3, and 6 using the ELISA-based HDAC activity assay.<sup>21</sup> All analogs were tested at 5  $\mu$ M concentration, except for 1d, which was tested at 10  $\mu$ M. SAHA was tested at 1  $\mu$ M.<sup>21</sup> Mean percent deacetylase activities from a minimum of three independent trials with standard errors were plotted (Table S2). The substituent below each compound number corresponds to the R group in C2-modified SAHA (Figure 1).

Figure 2

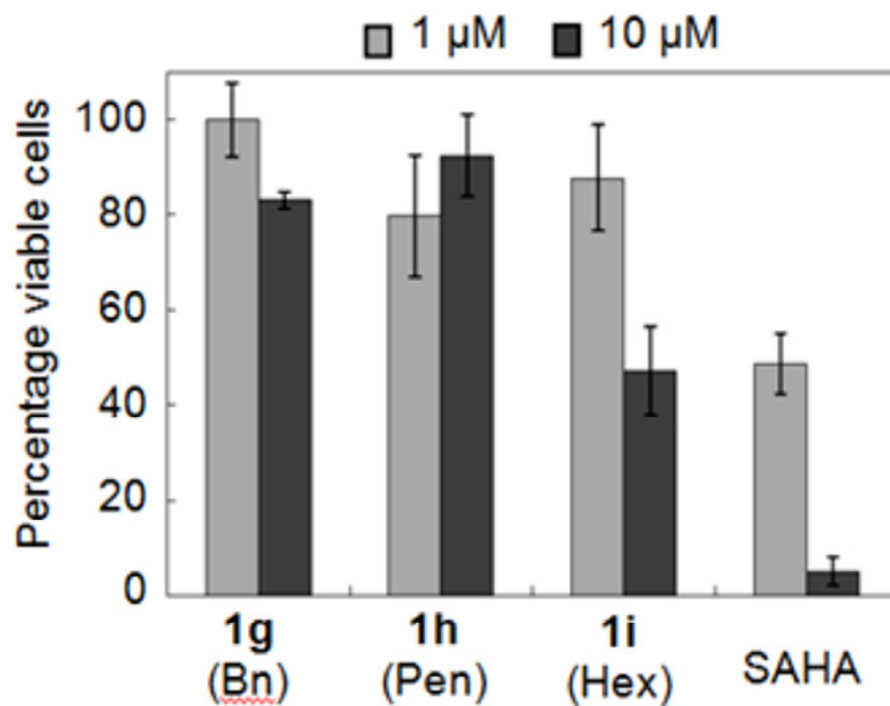
78x59mm (300 x 300 DPI)



Cell-based selectivity testing of the SAHA analogs. U937 cells were treated with (a) DMSO (1%), SAHA (2  $\mu$ M), tubastatin (2  $\mu$ M), C2-benzyl SAHA (1g, 30  $\mu$ M), C2-n-pentyl SAHA (1h, 30  $\mu$ M), C2-n-hexyl SAHA (1i, 30  $\mu$ M), or (c) increasing concentrations of C2-n-hexyl SAHA analog (1i, 10-60  $\mu$ M) before lysis, SDS-PAGE separation, and western blot analysis of acetyl-histone H3 (AcH3) and acetyl- $\alpha$ -tubulin (AcTub). GAPDH was a load control. Repetitive trials are shown in Figures S49 and S50. (b) Fold increase in AcH3 or AcTub after quantification of bands intensity from part a, with mean fold increase from four independent trials and standard error (Table S10).

Figure 3

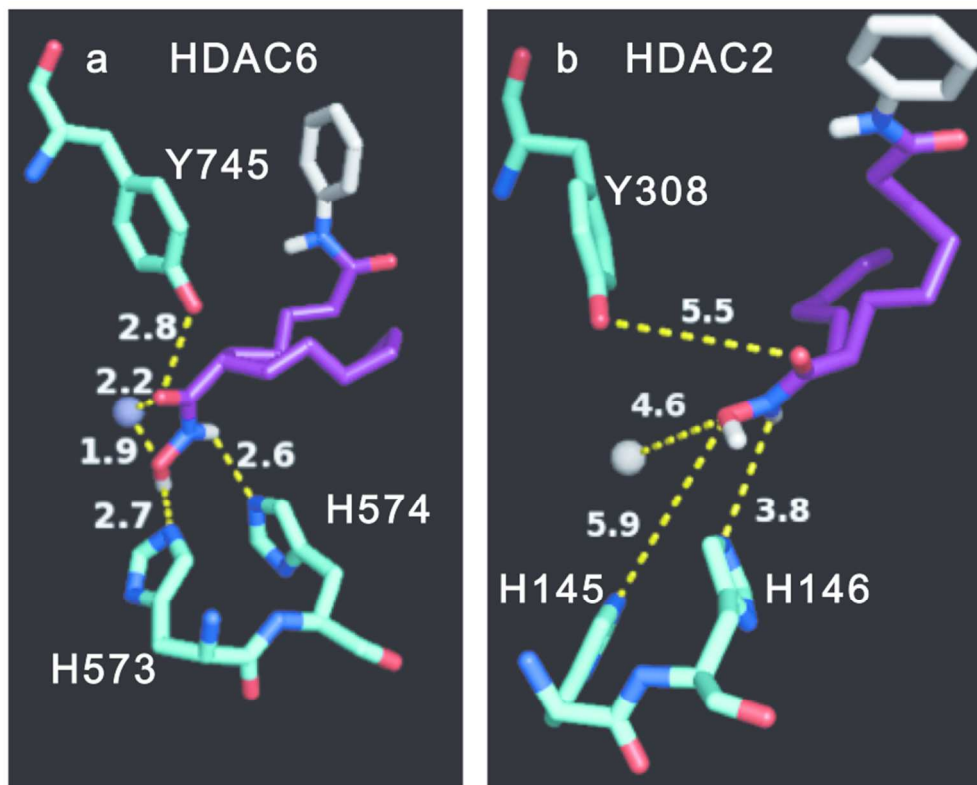
88x69mm (300 x 300 DPI)



Cytotoxicity screening of 1g, 1h, 1i, and SAHA at 1 and 10  $\mu\text{M}$  concentrations using an MTT assay with Jurkat cells. Mean percent viability from at least three independent trials with standard error were plotted (Table S11).

Figure 4

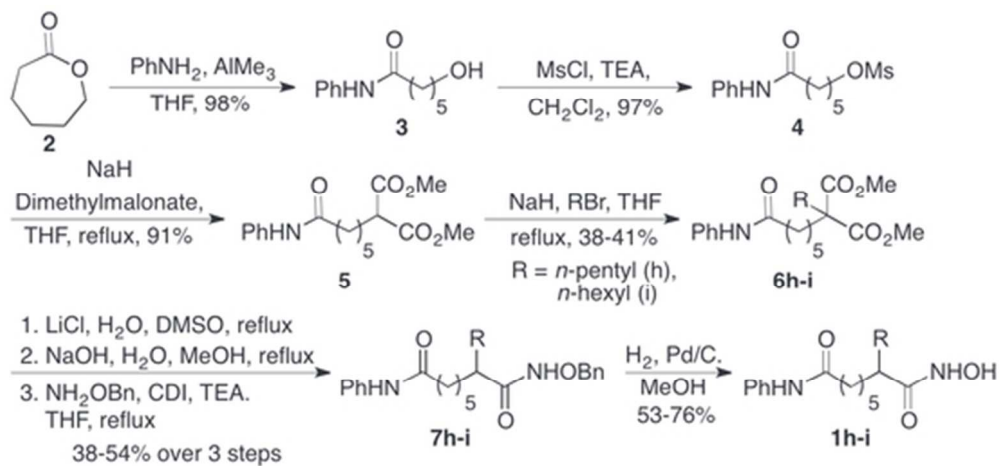
52x37mm (300 x 300 DPI)



Docked pose of (S)-C2-hexyl SAHA ((S)-1i) in the (a) HDAC6 (pdb:5EEM)<sup>34</sup> or (b) HDAC2 (pdb:3MAX)<sup>35</sup> crystal structures (b) using Autodock 4.2.33. Binding distances between the hydroxamic acid atoms and active site residues (numbered in figure) or the metal are displayed in Angstroms. The (R) enantiomer is shown in Figure S53. The atomic radius of the metal (Zn<sup>2+</sup>) was set at 0.5 Å for clarity. Atom color-coding: (S)-C2-n-hexyl SAHA (C=purple/white; O=red; N=blue; H=white); amino acids (C=deep teal; O=red, N=blue); Zn<sup>2+</sup> metal ion (grey sphere).

Figure 5

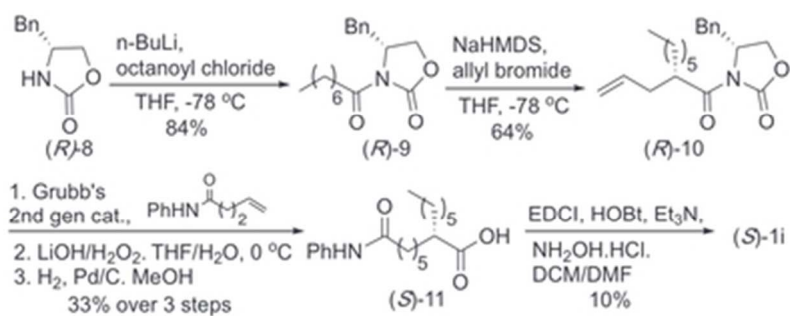
79x63mm (300 x 300 DPI)



Synthesis of C2-*n*-pentyl and C2-*n*-hexyl SAHA analogs (1h-i).

Scheme 1

46x22mm (300 x 300 DPI)



Synthesis of (S)-C2-n-hexyl SAHA, (S)-1i.

Scheme 2

33x13mm (300 x 300 DPI)